Thin Film Evaporation Using Nanoporous Membranes for Enhanced Heat Transfer

Citation: Xiao, Rong, Shalabh C. Maroo, and Evelyn N. Wang. "Thin Film Evaporation Using Nanoporous Membranes for Enhanced Heat Transfer." Proceedings of the ASME 2012 Summer Heat Transfer Conference, 8-12 July, 2012, Rio Grande, Puerto Rico, USA, ASME, 2012. © 2012 by ASME

As Published: http://dx.doi.org/10.1115/HT2012-58352

Publisher: ASME International

Persistent URL: http://hdl.handle.net/1721.1/120351

Version: Final published version: final published article, as it appeared in a journal, conference proceedings, or other formally published context

Proceedings of the ASME 2012 Summer Heat Transfer Conference
HT2012
July 8-12, 2012, Rio Grande, Puerto Rico

HT2012-58352

THIN FILM EVAPORATION USING NANOPOROUS MEMBRANES FOR ENHANCED HEAT TRANSFER

Rong Xiao
Department of Mechanical Engineering, MIT
Cambridge, MA, USA

Shalabh C. Maroo
Department of Mechanical & Aerospace Engineering,
Syracuse University
Syracuse, NY, USA

Evelyn N. Wang
Department of Mechanical Engineering, MIT
Cambridge, MA, USA

ABSTRACT

Recent advancements in integrated circuits demand the development of novel thermal management schemes that can dissipate ultra-high heat fluxes with high heat transfer coefficients. Previous study demonstrated the potential of thin film evaporation on micro/nanostructured surfaces [1-11]. Theoretical calculations indicate that heat transfer coefficients on the order of 10^6 W/m^{2}K and heat fluxes of 10^5 W/cm^2 can be achievable with water [1, 5-6]. However, in previous experimental setup, the coolant has to propagate across the surface which limits the increase in heat flux and the heat transfer coefficient, while adding complexity to the system design. This work aims to decouple the propagation of the coolant from the evaporation process through a novel experimental configuration. Thin nanoporous membranes of 13 mm diameter were used where a metal layer was deposited on the top surface to serve as a resistance heater. Liquid was supplied from the bottom of the membrane, driven through the nanopores by capillary force, and evaporated from the top surface. Heat transfer coefficient over 10^4 W/m^{2}K was obtained with isopropyl alcohol (IPA) as the coolant, which is only two orders of magnitude smaller than the theoretical limit. This work offers insights into optimal experimental designs towards achieving kinetic limits of heat transfer for thin film evaporation based thermal management solutions.

INTRODUCTION

Thermal management and heat dissipation has become a major limiting factor with the increase in computing power and reduction in size of the advanced integrated circuits (ICs). In recent years, the growth in power density of CPUs has flattened as the heat flux reaches 100 W/cm^2 [12], since existing thermal management approaches have difficulty in dealing with even higher heat fluxes. The further improvement of computing performance is mostly relying on the introduction of multi-core devices. The need for novel heat transfer schemes capable of dissipating heat fluxes over 100 W/cm^2 with a low temperature rise has been well-recognized.

A variety of phase-change based heat transfer schemes have been investigated including flow boiling in microchannel [13] and pool boiling on micro/nanostructured surfaces [14] which utilize the latent heat of vaporization to achieve high heat removal and efficient solutions. In these studies, the thin film evaporating region has been considered as the major contributor to the exhibited high heat transfer rates [1-9]. For example, Park et al. calculated that the maximum heat transfer coefficient at the thin film region in the meniscus can be as high as 100 MW/m^{2}K [10]. Similarly, Stephan and Busse [11] carried out numerical simulation to show that the local heat flux at the thin film region in grooves can be over 5000 W/cm^2. Therefore, thin film evaporation could be one of the most promising approaches to achieve the desired high heat fluxes and high heat transfer coefficients.

However, due to the difficulty in efficient liquid transport, peviously thin film evaporation has typically been demonstrated for local hotspot cooling [15]. In this work, we present using nanoporous membranes to achieve thin film evaporation over large areas. Heat transfer coefficient over 10^4 W/m^{2}K was obtained with isopropyl alcohol (IPA) as the coolant, which is higher than that of pool boiling and is only one order of magnitude smaller than the theoretical limit. This work offers insights into optimal experimental designs towards achieving kinetic limits of heat transfer for thin film evaporation based thermal management solutions.

NOMENCLATURE

A – Surface area of the membrane
f – Porosity of the membrane
h_{fg} – Latent heat of the liquid
h – Heat transfer coefficient
L – Thickness of the membrane

$\bar{M}$ – Molar mass
N –Total number of pores on the membrane
ΔP – Driving pressure across the membrane
P_{sat} – Saturation pressure
Q –Total heating power
q – Heat flux
R – Radius of the membrane
$\bar{R}$ – Molar gas constant
r – Radius of the nanopores
T – Temperature
T_{sat} – Saturation temperature
v_{lv} – Change in molar volume from liquid to vapor
μ – Viscosity of the liquid
ρ – Density of the liquid
$\hat{\sigma}$ – Accommodation coefficient

The nanoporous membranes used in our experiment was anodized aluminum oxide (Al_2O_3, Synkera Inc.) with diameter of 13 mm. The pore diameter was 150 nm. A 30 nm thick platinum layer was deposited on top of the membrane by sputtering, which was used as resistance heater as well as temperature sensor. The liquid was driven by capillary pressure as well as disjoining pressure through the pores to form the menisci, as shown in Fig. 1.

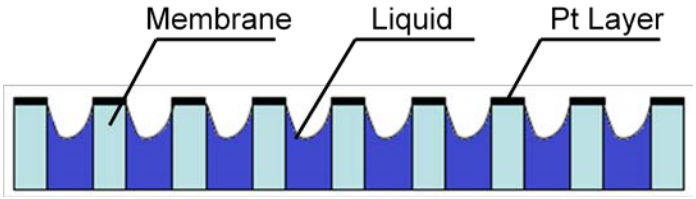

Fig. 1(a) Schematic showing the evaporation from nanoporous membrane.

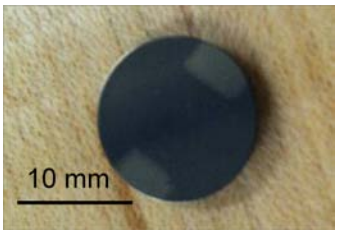

Fig. 1(b) The nanoporous membrane with Pt coating. The light-colored areas are contact pads where the pores are blocked with thicker Pt deposition.

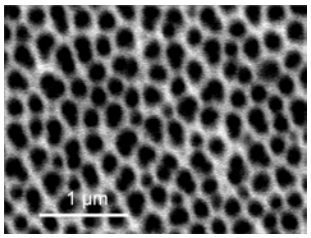

Fig. 1(c) Scanning Electron Micrograph (SEM) of the porous membrane. The pore diameters are around 150 nm and porosity is 31%.

During the experiment, the temperature was measured by the change in the resistance of the metal layer. However, due to the nanoscale geometry of the platinum layer and the sputtering fabrication process, the electrical property of the metal layer is different from that of the bulk material. Therefore, the temperature coefficient of resistivity was calibrated by an oven and a RTD thermal probe. The result of the calibration is shown in Fig. 2.

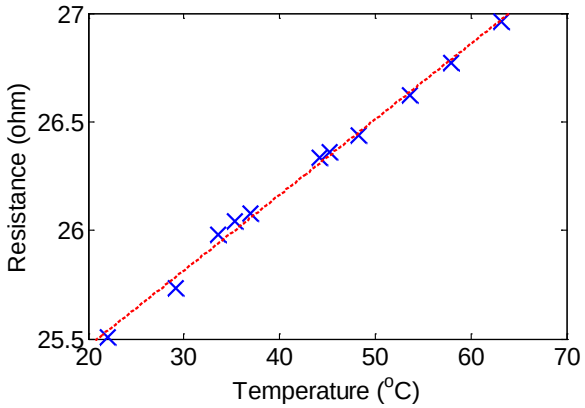

Fig. 2 The calibration of platinum resistor fabricated by sputtering. The temperature coefficient of resistivity was found to be 0.0014 K^{-1}.

The schematic of the experimental setup is shown in Fig. 3. During the experiment, vacuum conditions were maintained on top of the membrane using a vacuum pump in order to eliminate the effect of vapor diffusion in evaporation. The pressure over the membrane was controlled by a needle valve and measured by a vacuum gauge. On the bottom side of the membrane, the liquid was supplied using a syringe. The pressure of the bottom side was also controlled using a needle valve and measured by a vacuum gauge. A current was supplied to the metal layer which heated up the membrane. The voltage and current was measured by multimeters (Multimeter 2001, Keithley) and recorded by a computer using LabView (National Instruments) program such that the heating power and temperature were recorded. The data was acquired at a frequency of 1 Hz.

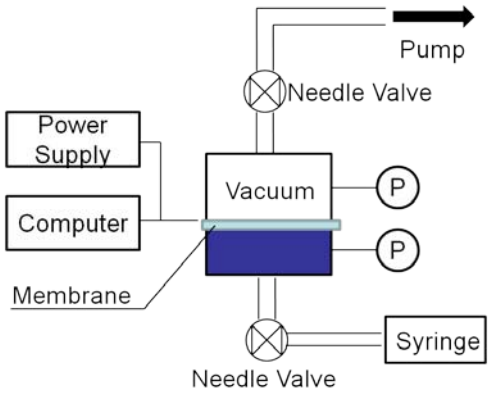

Fig. 3 Schematic of experimental setup.

The fixture in contact with the membrane was made of Ultem and vacuum was maintained using rubber o-rings, both of which have very low thermal conductivity. Therefore the heat loss into the fixture can be neglected. When the temperature of the membrane changed less than 1 degree over 100 seconds, we considered the surface to be in steady state, only after which the heating power was increased if needed.

The variation of the steady state temperature of the membrane with the increase in heat flux is shown in Fig. 4(a). Data was acquired using isopropyl alcohol (IPA) as the coolant. We used IPA instead of water due to the low surface tension of IPA, which allows wetting of the membrane even when the membrane gets contaminated and become less hydrophilic. Future effort will be focused on fabricating surfaces with robust hydrophilicity. As seen from Fig. 4(a), the initial heat transfer coefficient was relatively low with low heat flux. This is because at the early stage, the liquid flow driven by the pressure difference is higher than the evaporation rate. The top surface of the membrane was flooded by the excessive amount of liquid, which introduced a large thermal resistance. As the heat flux was increased, the evaporation rate became higher than the flow rate driven by pressure difference and the excessive amount of liquid on the surface on the membrane evaporated. The heat transfer coefficient increased significantly as the liquid menisci receded back into the pores and formed thin film regions. With further increase in the heat flux, the menisci shape yielded larger thin film regions resulting in the continuous increase of the heat transfer coefficient. At this stage of highest heat transfer coefficient, the liquid was driven through the pores by a combination of the pumping pressure, the capillary pressure and the disjoining pressure. However, with further increase in the heat flux, the total driving pressure was no longer able to supply enough liquid for evaporation, and the membrane started to dry out with significant rise of the membrane temperature The whole dynamic process of the liquid menisci is shown in Fig. 4(b)-(d).

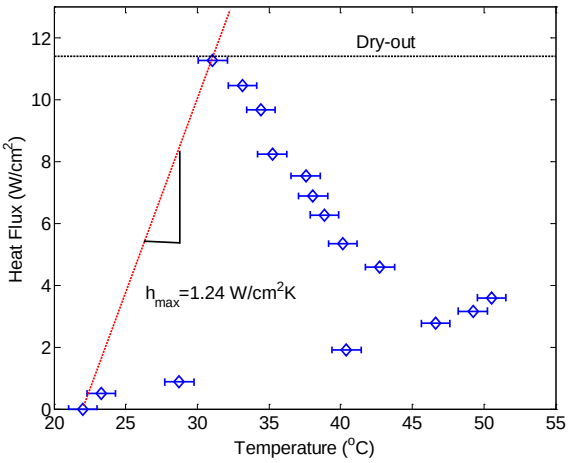

Fig. 4(a) One example showing the relation between heat flux and the temperature. The maximum heat transfer coefficient was 1.24 W/cm^2 at the heat flux of 11.38 W/cm^2. The working temperature was 31 ºC, which is significantly lower than the saturation temperature at the working pressure.

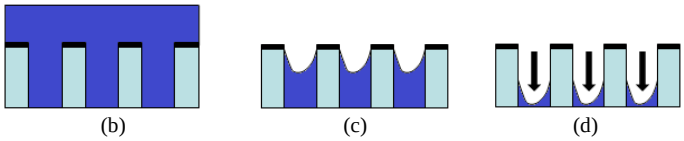

Fig. 4 (b) The flooding of the membrane with low heat fluxes; (c) High heat transfer coefficient provided by large thin film regions with medium heat fluxes; (d) Dry-out of membrane with high heat fluxes.

The overall maximum heat transfer coefficient achieved was 1.24 W/cm^{2}K. Based on kinetic theory [16], the theoretical limit of heat transfer coefficient for IPA at the conditions of the experiment can be determined as

$$h_i = \left(\frac{2\hat{\sigma}}{2-\hat{\sigma}}\right)\left(\frac{h_{fg}^{\ 2}}{Tv_{lv}}\right)\left(\frac{\bar{M}}{2\pi\bar{R}T}\right)^{\frac{1}{2}}\left(1-\frac{Pv_{lv}}{2h_{fg}}\right) \approx 458.11 W/cm^2K$$

The accommodation coefficient used in above calculation was assumed to be 0.03 [16, 17]. We can see that the heat transfer coefficient achieved in our experiment is only two orders of magnitude smaller than the theoretical limit. The major reason to the difference between experiment value and theoretical limit is that the experiment was not carried out under saturation conditions. Therefore the diffusion of vapor molecule contributes to the thermal resistance significantly. Moreover, the actual thin film area is still much smaller than the overall surface area, which also reduces the experimental heat transfer coefficient.

As started earlier, in our experiment, the liquid was supplied by the combination of vacuum pressure by pumping, the capillary pressure and disjoining pressure. The magnitude of the capillary pressure and disjoining pressure can be estimated based on the maximum heat flux when the dry-out happens. Since the heat loss into the fixture is negligible, the evaporation rate and the average velocity of liquid flowing in the nanopores can be determined by an energy balance as follows:

$$\dot{m} = \frac{Q}{h_{fg}}$$

The liquid flow was driven by the balance between the driving pressure and the viscous resistance

$$\frac{\Delta P}{L} = \frac{8\mu}{r^4}\frac{\dot{m}}{\rho N}$$

where

$$N = \frac{\pi R^2 f}{\pi r^2}$$

Therefore, the total amount of heat dissipated through evaporation is determined by the driving pressure

$$Q = \frac{\pi r^2 R^2 f \rho h_{fg} \Delta P}{8\mu L}$$

The maximum heat flux can be determined as

$$q = \frac{r^2 f \rho h_{fg} \Delta P}{8\mu L}$$

Given the physical properties of IPA, the relation between the maximum heat flux and the total driving pressure is plotted in Fig. 5.

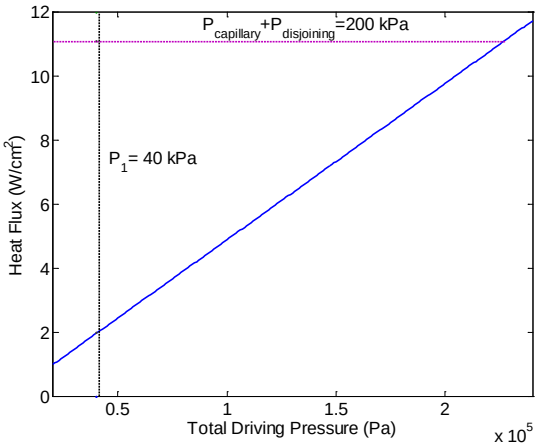

Fig. 5 Maximum heat fluxes as a function of the total driving pressure. P_1 is the pressure provided by the pumping. In the experiment shown in Fig. 4, the maximum heat flux was 11.38 W/cm^2, corresponding to capillary pressure and disjoining pressure combined to be 200 kPa.

As shown in Fig. 5, a combined driving pressure of 200k Pa was achieved in our current experiment. Considering the pressure of the reservoir is at atmosphere, the pressure near the menisci is around -140 kPa. Such large negative pressure was possible due to the nanoscale confinement by the pores, which prohibits cavitation and allows the liquid to exist in the metastable state [18]. Similar phenomenon has been found in trees where the large negative pressure enables the transport of water from the root to the leaves. Synthetic trees using nanoporous membranes to create large negative pressure to achieve high-efficiency water transport have also been demonstrated [19]. However, the application of such phenomenon in practical engineering systems has yet to be fully exploited. In this work, we have demonstrated a possible application for high heat flux thermal management. Current heat fluxes are relatively low due to the large viscous resistance and long liquid transport distance. In the future, thinner membranes will be tested to enhance the maximum heat flux. For example, by simply reducing the thickness of the membrane from 100 to 10 μm, the maximum heat fluxes can potentially be increased by 10 times, which would be able to meet the thermal management challenges of 100 W/cm^2.

In conclusion, we demonstrated a system where nanoporous membranes were used to generate large negative pressures and attain high heat transfer coefficients. The negative pressure enables efficient transport of liquid for evaporative heat transfer. Thin film evaporation allowed for heat transfer coefficient to be only two orders of magnitude smaller than the kinetic limit. Such systems incorporating nano-thin film evaporation hold significant potential in addressing thermal management challenges for advanced electronic devices.

ACKNOWLEDGMENTS

The authors gratefully acknowledge funding support from the Office of Naval Research (ONR) with Dr. Mark Spector as program manager and the MIT Martin Family Fellowship. The authors also thank the MIT Microsystems Technology Lab (MTL) for fabrication staff support, help and use of equipment.

REFERENCES

[1] H. Wang, S.V. Garimella, and J.Y. Murthy, "Characteristics of an evaporating thin film in a microchannel", *International Journal of Heat and Mass Transfer*, Vol. 50: pp. 3933-3942, 2007

[2] S.J.S. Morris, "The evaporating meniscus in a channel", *Journal of Fluid Mechanics*, Vol. 494 pp. 297–317, 2003

[3] H.B. Ma, G.P. Peterson, "Temperature variation and heat transfer in triangular grooves with an evaporating film", *Journal of Thermophysics and Heat Transfer*, Vol. 11 pp. 90–97, 1997

[4] B. V. Deryagin, S. V. Nerpin, and N.V. Churayev, "Effect of film transfer upon evaporation of liquids from capillaries", *Bull. R.I.L.E.M.*, 29: p. 93-98, 1965

[5] M. Potash jr., P. C. Wayner Jr., "Evaporation from a two-dimensional extended meniscus", *International Journal of heat and Mass Transfer*, Vol. 15, pp. 1851-1863, 1972

[6] P. C. Wayner Jr., Y. K. Kao, L. V. LaCroix, "The interline heat transfer coefficient of an evaporating wetting film", *International Journal of heat and Mass Transfer*, Vol. 19, pp. 487-492, 1976

[7] K.P. Hallinan, H.C. Chebaro, S.J. Kim, W.S. Chang, "Evaporation from an extended meniscus for nonisothermal interfacial conditions", *Journal of Thermophysics and Heat Transfer*, Vol. 8, pp. 709–716, 1994.

[8] S. DasGupta, J.A. Schonberg, P.C. Wayner Jr., "Investigation of an evaporating extended meniscus based on the augmented Young–Laplace Equation", *Journal of Heat and Mass Transfer*, Vol. 115 pp. 201–208, 1993

[9] J.B. Freund, "The atomic detail of an evaporating meniscus", Physics of Fluids, Vol. 17 022104, 2005

[10] K. Park, K. Noh, K. Lee, "Transport phenomena in the thin-film region of a micro-channel", *International Journal of Heat and Mass Transfer* Vol. 46 pp. 2381–2388, 2003

[11] P.C. Stephan, C.A. Busse, "Analysis of the heat transfer coefficient of grooved heat pipe evaporator walls", *International Journal of Heat and Mass Transfer*, Vol. 35 pp. 383–391, 1992

[12] E. Pop "Energy dissipation and transport in nanoscale devices", *Nano Research*, Vol. 3(3), pp. 147-169, 2010

[13] S. G. Kandlikar, "Fundamental issues related to flow boiling in minichannels and microchannels", *Experimental Thermal and Fluid Science*, Vol. 26, pp. 389-407, 2002

[14] B. R. Babin, G. P. Peterson, D. Wu, "Steady-state modeling and testing of a micro heat pipe", *Journal of Heat Transfer*, Vol. 112:3, pp. 595-601, 1990

[15] S. Narayanan, A. Fedorov, Y. K. Joshi, “On-chip thermal management of hotspots using a perspiration nanopatch”, *Journal of Micromechanics and Microengineering*, Vol. 20(7), 075010, 2010
[16] V. P. Carey, “Liquid-Vapor Phase-Change Phenomena”, Hemisphere Pub. Corp., 1992
[17] B. Paul, “Compilation of evaporation coefficients”, *ARS J.*, Vo. 32, pp. 1321-1328, 1962
[18] Shalabh C. Maroo & J. N. Chung, Negative pressure characteristics of an evaporating meniscus at nanoscale, *Nanoscale Research Letters*, 6:72 (2011)
[19] T.D.Wheeler, A.D.Stroock, “The transpiration of water at negative pressures in a synthetic tree”, *Nature*, 455, 208-212, 2008